Received 24 April 2024; revised 28 June 2024; accepted 16 July 2024. Date of publication 18 July 2024; date of current version 24 September 2024.

Digital Object Identifier 10.1109/OJAP.2024.3431092

Preliminary Design and Test of a Microwave Inline Moisture Sensor for the Carasau Bread Industry

GIACOMO MUNTONI [1] (Member, IEEE), MATTEO B. LODI [1] (Member, IEEE), ALESSANDRO FEDELI [2] (Member, IEEE), ANDREA MELIS [1], CLAUDIA MACCIÒ [1], MATTEO PASTORINO [2] (Fellow, IEEE), ANDREA RANDAZZO [2] (Senior Member, IEEE), GIUSEPPE MAZZARELLA [1] (Senior Member, IEEE), AND ALESSANDRO FANTI [1] (Senior Member, IEEE)

[1]Department of Electric and Electronic Engineering, University of Cagliari, 09123 Cagliari, Italy

[2]Department of Electrical, Electronic, Telecommunications Engineering and Naval Architecture, University of Genoa, 16145 Genoa, Italy

CORRESPONDING AUTHOR: A. FANTI (e-mail: alessandro.fanti@unica.it)

This work was supported in part by tMinistero dello Sviluppo Economico, in AGRIFOOD Programma Operativo Nazionale (PON) Imprese e Competitività (I&C) 2014–2020 through the Project "Ingegnerizzazione e Automazione del Processo di Produzione Tradizionale del Pane Carasau mediante l'utilizzo di tecnologie IoT (IAPC)" under Grant CUP: B21B19000640008 COR: 1406652, and in part by the Italian Ministry of Enterprises and Made in Italy (MIMIT), within the "ACCORDI PER L'INNOVAZIONE" (2021–2026) through the Project AISAC under Grant CUP: B29J23001120005 – COR: 1607797.

This article has supplementary downloadable material available at https://doi.org/10.1109/OJAP.2024.3431092, provided by the authors.

ABSTRACT Within the framework of the recent agri-food technological advancement, the design and validation of a methodology for the water content estimation in the Carasau bread manufacturing process is herein presented. Following a thorough evaluation of the dough dielectric properties, a suitable antenna layout has been selected, pointing out the advantages in the choice of a contactless narrow-band antenna in comparison to wide-band and dual-band ones. The presented simulated results are then validated using a prototype sensor and an ad hoc measurement system to confirm the antenna ability to discriminate among doughs with different water content. In addition, an accurate analysis of possible sources of misinterpretation of the results is presented.

INDEX TERMS Dielectric properties, moisture sensor, Carasau bread, patch antenna, food engineering.

I. INTRODUCTION

WITHIN the branch of microwave non-communication applications, the agri-food sector is witnessing a high-paced technological advancement. Through microwave technology, wireless sensors are proficiently employed for food dielectric characterization [1], grains and fruit quality inspection [2], [3], [4], adulteration and contamination detection [5], [6], [7], and traceability [8], [9]. The convenience of automating such processes also affects productions that are intrinsically antithetical to large-scale industrial advancements, like traditional bakery. Traditional food is the backbone of Italian cuisine, and it is so rooted in its history that each region boasts countless typical products. One example is the Carasau bread, a thin, crunchy traditional Italian bread made in Sardinia [10]. The Carasau bread industry has already started a technological advancement. Indeed, recently, a novel wireless sensor network able to monitor several parameters (i.e., ambient temperature, relative air humidity, CO and CO_2 concentration, speed of the conveyor belt, morphology and texture of the bread) at every production step [11], and a blockchain-based traceability system [12] have been developed. Nonetheless, a dedicated sensor or a disruptive methodology for quality inspection in early production stages is still missing.

Carasau bread is made from re-milled semolina of durum wheat, sea salt, natural yeast, and de-chlorinated drinking water [13]. The production chain includes kneading, leavening, sheeting, and baking stages, which will be better explained in Section II. It is worth noting that one of the most important passages in the bread production is between the leavening and baking stages, wherein the dough must have the proper water content ($W_{\%}$) to secure a successful

baking [14], [15]. Otherwise, the final product could be defected, rising the overall production cost to compensate the waste. This analysis is the result of a survey in a real Carasau bakery located in Fonni (NU), central Sardinia, Italy. As an example, to justify the urge of a reliable sensing system, the latter bakery reports an amount of wasted product, due to inaccuracy of water content in the dough, equal to 300 kg per day, which is equal to about 12% of the total production. With this industrial stakeholder, the following system requirements have been set: i) cost-effectiveness, ii) easy deployment, iii) be able to sense water content variation between 46% and 54%, in a robust and sensitive way. To date, in the literature, rheological [16], nuclear magnetic resonance [17] and Fourier transform infrared (FTIR) measurements [18] were proposed as methodologies for assessing the quality and composition of Carasau bread doughs. However, these quantitative approaches require expensive and cumbersome equipment, with a non-trivial result interpretation (calling for expert users), and demand a specific sample preparation, thus being not suitable for in-line inspection. This is why, recently, broadband dielectric spectroscopy in the range 1 Hz-10 MHz, performed at cryogenic temperatures, was investigated as a potential alternative methodology [19]. However, common devices and tools used for dielectric spectroscopy (e.g., open-ended coaxial probe, resonant cavities, etc.) cannot be used in industrial settings, requiring contact with sample, being invasive or determining a potential contamination of the food product. Actually, despite being somehow a niche topic, already published literature dealt with general improvement of the Carasau production chain but with no dielectric characterization of the product [10], [11], quantitative methodologies for quality and dielectric composition assessment of the dough but very expensive and more suitable for a laboratory than an industrial production line [16], [17], [18], dielectric characterization of the dough that, however, cannot be applied in an inline scenario [19], and dielectric characterization of the sheeted dough based on the amount of water that cannot rely on real measurement to support its conclusions [13]. This latter aspect needs further investigations.

In this perspective, it is clear the necessity to develop a robust, cost-effective and electromagnetic-based (contactless) methodology for measuring the water content in the production chain between the leavening and baking steps, so a suitable device that can be easily integrated in the proximity of the conveyor belt. Such methodology, unprecedented in the open scientific literature due to its specific product-related nature, should consist of an antenna sensor that, in a contactless way, is able to sense a difference in permittivity among doughs with different water content. The antenna is assumed to be located in a fixed position, taking advantage of the movement of the conveyor belt, to analyze every unbaked bread sheet being transported. This system takes advantage of the modification of the antenna resonance due to the different permittivity of the dough, which depends on the water content.

Microwave sensors based on microstrip technology are amongst the most employed for permittivity [20], and humidity/moisture detection, preferable, for instance, to destructive and invasive methods such as the coaxial probe [21]. They can be employed in several fields of application, such as humidity evaluation in soils [22], [23], [24], [25], [26], and in food and food-related products [2], [3], [27], [28], [29]. Many examples are reported, in the open literature, of water content sensors relying on microstrip patch antennas for their low cost and low profile [25], [30], [31], [32]. However, most of these sensors operate in direct contact with the Material Under Test (MUT), a solution that must be avoided in the presented scenario. In the case of the Carasau bread, a suitable inline microwave sensor should be taken into account to be fully integrated into the production chain, maintaining a proper clearance between the antenna and the bread sheet, and acquiring the moisture data in a non-destructive way.

In this work, the design, numerical simulations, and validation of a new methodology for a contactless inline microwave sensing of Carasau bread sheet moisture is presented. Aim of the paper is to assess what type of antenna layout is the best choice for the presented measurement scenario and satisfy the industrial requirements. In particular, we focused on the sensor capability of discriminating small percentages variation ($\sim$4%) of water content inside the Carasau dough. A thorough numerical investigation had to be carried out to understand if the existing difference in permittivity was even measurable.

We selected some representative test cases, agreed with our industrial stakeholders and the specific needs of this production. The first phase of the study has been focused on the measurement of the complex dielectric permittivity of the dough with different $W_{\%}$ (46%, 50%, and 54% w.r.t. the total weight of the semolina). A commercial open-ended coaxial probe has been used for the measurements. However, since the probe cannot be used for inline measurement and is an invasive and destructive method, a suitable microwave sensor has to be placed between the second leavening and baking steps (see Fig. 1 for reference and consult Section III of the supplementary material). Thus, the second phase included the setup of the simulation environment and the choice of the antenna layout. Based on a direct comparison between wide-band, dual-band, and narrow-band antennas, it has been found that only the latter offer a fair discrimination of the moisture variation. A simple, but effective, coaxial-fed microstrip patch antenna has been chosen, accordingly. The selection of the operating frequency has been dictated by the small-scale industrial environment (which limited the available bandwidths to the ISM frequencies, according to European directive 2006/42/CE) and by the intrinsic dielectric characteristics of the dough. Therefore the 5.8 GHz ISM band has been chosen.

The simulations results highlight that a simple patch antenna close enough to the bread sheet can discriminate the

$W\%$ based on the magnitude difference of the S_{11} minima. To endorse this statement, a set of measurements has been performed using an *ad hoc* setup. Despite the discrepancy between the simplistic numerical environment (preferred for a light computational load) and the dedicated measurement setup, a good agreement has been found in the comparison. In addition to the validation of the methodology, a further study has been conducted to assess the robustness of the presented system to factors unrelated to the variation of water content. These factors include geometrical variation to the envisioned scenario, such as changes in the antenna-sheet distance and changes in the sheet thickness.

The paper is organized as follows:

- Section II is devoted to the explanation of the Carasau bread manufacturing process, highlighting its key aspects and the dough ingredients.
- Section III describes the characterization of the Carasau dough using a commercial coaxial probe to derive the general dielectric profile to be used in the simulations, as well as retrieving how the dielectric properties vary with water content.
- Section IV delves into the choice of the antenna layout suitable for the contactless characterization of the sheeted dough and presents the electromagnetic simulations of the coupling between the chosen antenna and the sheeted dough with different water content.
- Section V outlines the fabrication of the prototype used for the measurements, describes the measurement setup used, and shows the comparison between simulated and measured results.
- Section VI warns about potential causes of misinterpretation of the results and how to recognize them with further comparisons between simulations and measurements.
- Section VII draws the conclusion of the work and suggests a possible employment of the data retrieved in this study.

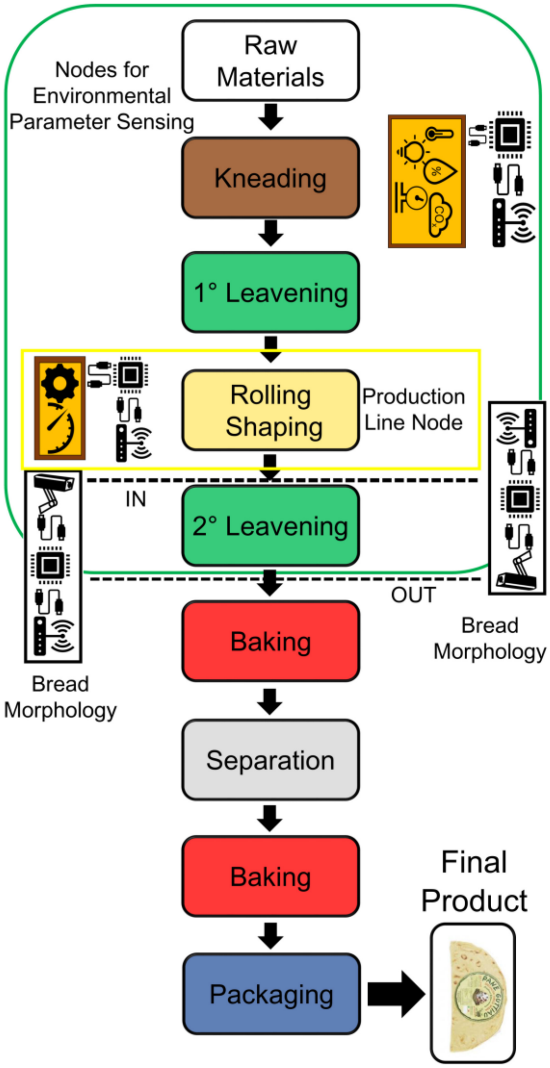

FIGURE 1. Schematic representation of the Carasau bread baking process.

II. CARASAU BREAD MANUFACTURING PROCESS

The production process of the Carasau bread starts from raw materials: re-milled semolina of durum wheat, sea salt, natural yeast, and de-chlorinated tap water. The ingredients are mixed inside a kneading machine and converted into dough that has to leaven at a temperature of 28-32°C [10], [11], [12], [13], [14], [15], [16], [17], [18]. Next, the dough is sheeted by a machine and disks of 36 cm in diameter are obtained (actually, the disks are not perfectly circular, as it is pointed out in Section IV). Then, the disks are transported in a dedicated leavening room by the conveyor belt, wherein they undergo a second session of leavening. It follows a first baking at 570 °C in an oven, after which the disks are left to cool for around 5 minutes and then separated manually by trained operators to obtain two sheets. Lastly, the latter are baked again at 400 °C to obtain the final product. A schematic representation of the Carasau bread baking process is reported in Fig. 1.

III. COMPLEX DIELECTRIC PERMITTIVITY OF CARASAU BREAD DOUGH AND SHEET

The methodology for obtaining the relative complex dielectric permittivity, $\epsilon(f) = \epsilon' - j\epsilon''$, of the Carasau dough was re-adapted from [19]. These measurements have been performed primarily in order to model the sheeted dough within the CST simulation environment. The measurement setup included the commercial DAK 3.5 Speag open-ended dielectric probe connected to the Rhode & Schwarz vector network analyzer (VNA) VN8. The frequency range has been set between 0.5 and 8 GHz, using a 50 MHz span. The measurements results are presented as the average value of 10 measurements, considering the standard deviation and the combined standard deviation. They have been performed on small dough samples inserted in suitable sample holders.

The standard recipe for the Carasau bread dough consists of 4.5 g of salt, 4.5 g of yeast, 300 g of semolina, and 150 g of water (50% of $W_{\%}$ w.r.t. the total weight of the semolina). In order to mimic the excess or defect of water

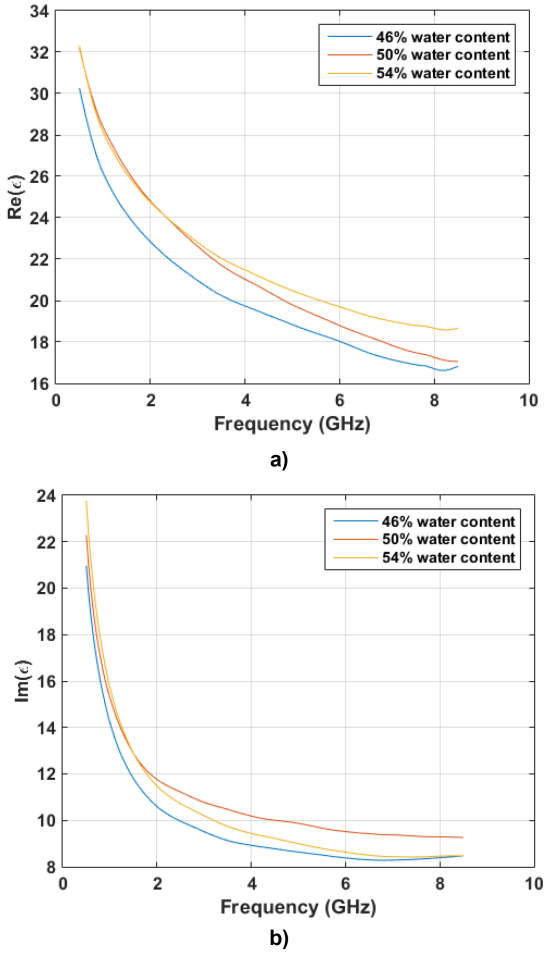

FIGURE 2. Preliminary measurements of the real (a) and imaginary (b) part of the complex dielectric permittivity for the Carasau bread dough with different water content.

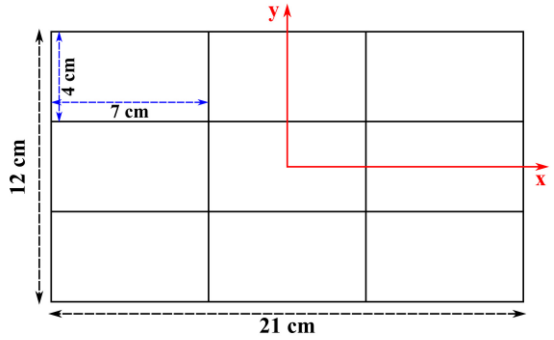

FIGURE 3. Schematic of the grid considered for acquiring dielectric measurements over the Carasau dough samples.

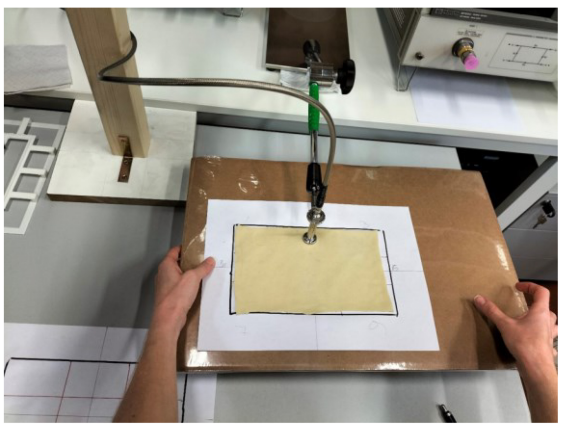

FIGURE 4. Picture of the measurement process using the coaxial probe connected to the VNA (Rhode & Schwarz ZNB 8).

typically encountered during the bakery operations [10], [11], [12], [13], [14], [15], [16], [17], [18], the recipe has been modified by altering the percentage of water to 54% and 46%, respectively. After the required steps of kneading (20 min) and first leavening (40 min), part of the dough has been used to create the small samples for the probe measurements, whereas the remaining part of the dough has been manually sheeted using a pasta machine, reaching the desired thickness of about 1 mm, to match the real industrial sheets. According to the preliminary measurements on the small dough samples with 46%, 50%, and 54% $W_{\%}$, a relevant difference in both real and imaginary part of the complex dielectric permittivity is found between 4 and 6 GHz, as shown in Fig. 2. Consequently, the ISM operating frequency of 5.8 GHz has been selected. The values reported in Fig. 2 have been used to model the dielectric profile of the sheeted dough within the CST simulation environment.

After having identified a suitable working frequency in which the dielectric contrast is relevant, the sheeted dough has been cut into 21 cm x 12 cm rectangular samples. This experiment has been performed in order to understand if there was a large disparity of $W_{\%}$ in the same sheet. The effective dielectric properties of each sample have been evaluated in different positions of the sheeted dough by considering a 3 x 3 grid, in order to map the spatial distribution of the relative effective[1] complex permittivity (i.e., $\epsilon_r(x, y)$). In this way, we aimed at evaluating the spatial diversity and level of homogeneity of the sheets. In fact, the different $W_{\%}$ would affect the dough texture and impact on the drying process, with effects on the final product quality [33]. Each rectangular element of the considered grid has size 4 cm x 7 cm, as reported in the schematic in Fig. 3. A picture of the measurement process is reported in Fig. 4. The measurement of $\epsilon_r(x, y)$ has been made by placing the probe in the center of each grid rectangle.

The results of the effective complex permittivity measurements of the samples for the considered $W_{\%}$ at 5.8 GHz are shown in Fig. 5a, 5b, and 5c. The Carasau dough sheet with 46% $W_{\%}$presents a more spread distribution of both ϵ' and ϵ'' ($\pm$ 0.1 unit of permittivity per cm^2) with respect to the other 2 cases, though it is still contained. Indeed, as the water content increases, the deviation of the complex permittivity decreases, and the dough sheets at 50% and 54% becomes very homogeneous ($\sim \pm$ 0.01 unit of permittivity

[1]Note that the term effective has been used to take into account also possible contribution from the materials below the sheeted samples.

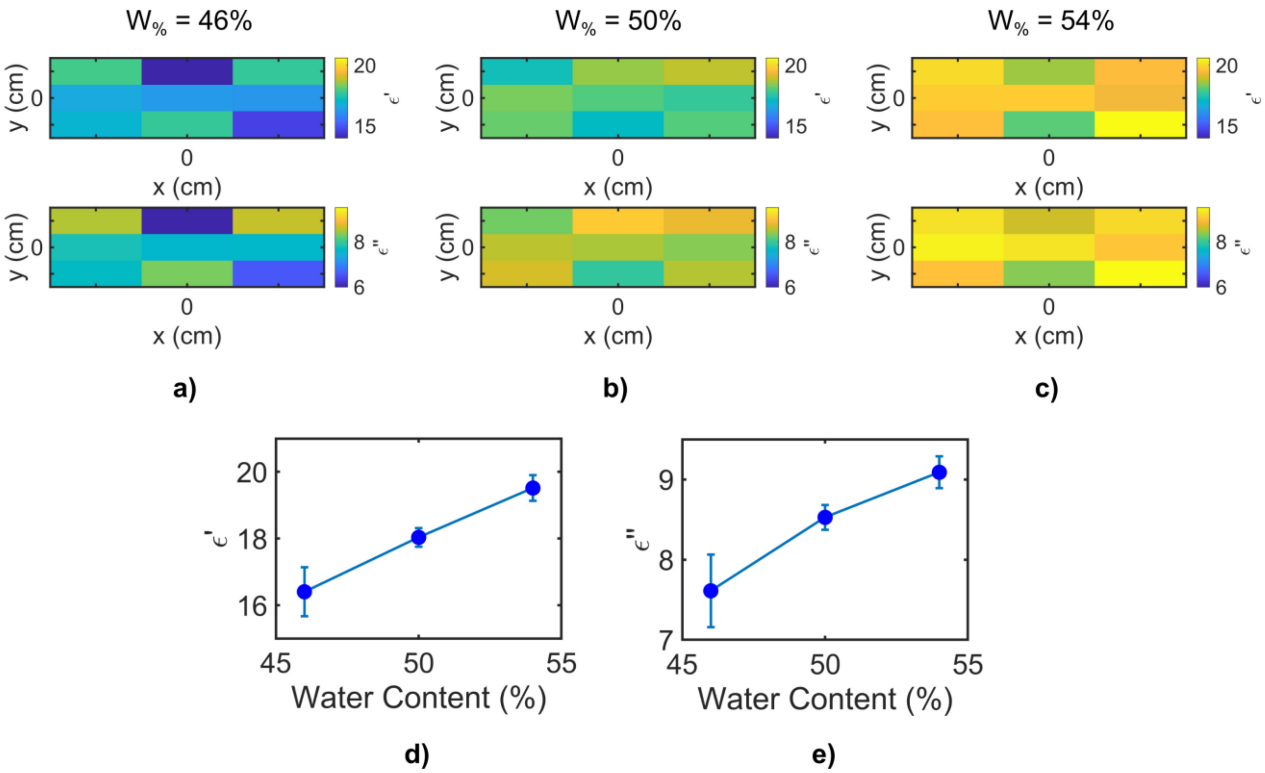

FIGURE 5. Distribution of the relative complex permittivity for the rectangular sample with 46% (a), 50% (b), and 54% $W_{\%}$ (c), and average complex permittivity (real – d, and imaginary – e) for the rectangular sample with respect to $W_{\%}$ variation at 5.8 GHz.

per cm^2). The average effective complex permittivity for the $W_{\%}$ variation at 5.8 GHz and the relative standard deviation are also reported in Fig. 5d and 5e. Based on these findings, we can conclude that the permittivity profile, within the same sheet, is pretty much uniform. This allows us to hugely simplify the simulations, as we could model the dough sheets with a dielectric profile that changes with frequency but not with space.

IV. CHOICE OF THE ANTENNA DESIGN AND SIMULATIONS

In order to select the proper layout for the envisioned measurement methodology and satisfy the system requirements given by the industrial stakeholder, different types of antennas have been simulated, testing the sensitivity, with respect to the $W_{\%}$ variation, of wide-band, dual-band, and narrow-band antennas.

To choose which type of antenna could be suitable for this application, the authors decided to divide the antennas to be tested into classes based on a bandwidth criterion, rather than show countless layouts with the same outcome, and highlight the simplest ones (easily reproducible). Basically, more than one antenna for each class has been tested but for the sake of simplicity, since the conclusion is arguably the same for each antenna in the same class, we opted to show one representative case. The wide-band antenna is a WR 187 pyramidal horn antenna whose dimensional drawing is reported in Fig. 6. The waveguide section of the

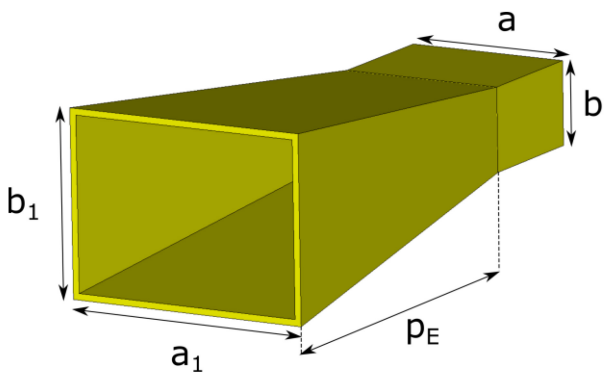

FIGURE 6. Dimensional drawing of the WR 187 pyramidal horn antenna. Parameters: a = 47.55 mm, b = 22.15 mm, a_1 = 73.4 mm, b_1 = 53.85 mm, p_E = 139.7 mm.

pyramidal horn is a WR 187, thus with size 47.55 mm x 22.15 mm. The a_1 x b_1 aperture (with $a_1 = 73.4$ mm and $b_1 = 53.85$ mm) is spaced out from the feeding waveguide by $p_E = 139.7$ mm. A summary of the horn dimensions is reported in the caption of Fig. 6. The dimensional drawing of the dual-band patch antenna is reported in Fig. 7. The dual-band antenna is a series fed stacked patch with both substrates made of Polylactic Acid (PLA, $\varepsilon_r = 2.54$, $\tan\delta = 0.015$) having thickness $h = 1$ mm and size S x S (with $S = 50$ mm). The substrates are separated by a small gap $g = 0.5$ mm. The bottom parasitic patch size is $W1$ x $L1$ (with $W1 = 22$ mm and $L1 = 18.25$ mm), whereas the top radiating patch size is W x L (with $W = 24$ mm and $L =$

18.5 mm). Both patches are made of copper. The coaxial feed is located at $x_f = 4.8$ mm from the center of the patch. A summary of the series fed stacked patch dimensions is reported in the caption of Fig. 7. Finally, the narrow-band antenna (resonating at 5.8 GHz) is a simple coaxial-fed patch, having a PLA S_p x S_p x h_p substrate (with $S_p = 35$ mm and $h_p = 2$ mm). The PLA has been chosen to speed up the prototyping process with 3D-printing, in preparation for the validation measurements. The copper patch has size W_p x L_p (with $W_p = 19.54$ mm and $L_p = 15.15$ mm) and the feeding point is placed at $x_{fp} = 3$ mm from the center of the patch (for a summary of the dimensions of the 5.8 GHz patch, please refer to the caption of Fig. 12, where the simulation environment is reported).

For comparison, the magnitude of the input reflection coefficient ($|S_{11}|$) in free space for the three layout is displayed in Fig. 8, highlighting the difference in bandwidth between the three antennas.

The simulation environment for the moisture sensitivity has been built in the CST Studio Suite workspace and consists of the antenna for the $W_{\%}$ estimation, placed above the bread sheet, which is in direct contact with a rubber conveyor belt (see Fig. 12 for reference). The default distance between the antenna and the bread sheet has been chosen equal to $d = 10$ mm. In this respect, shorter distances improve the overall sensitivity of the sensor and the chosen value is the lowest one that does not hinder the baking process. The shape and size of the Carasau bread sheet has been derived from several measurements on samples from a real traditional bakery. It has been chosen of elliptical shape with axis equal to 370 mm and 360 mm, and thickness equal to 1 mm, since the unbaked bread sheets do not have a perfect circular shape. The selected simulation environment is rather simple but convenient, without additional components that would burden the computational load of the simulation. Aim of these simulations is simply to verify if the sensor is capable of discriminating the difference in $W_{\%}$, whereas the real validation of the presented point is entrusted to the measurements. A total of three simulation have been carried out, accounting, respectively, for the horn, the stacked patch and the 5.8 GHz patch antennas as the moisture sensor for a Carasau dough sheet with different $W_{\%}$ (46%, 50%, and 54%).

In Figs. 9 and 10, the frequency response of the first two cases is studied. From the images, it is clear that these layouts are pretty much unsusceptible to the variation of water inside the dough. The shift of the $|S_{11}|$ curve is barely visible in both cases. To be more precise, the maximum difference in magnitude between the highest and the lowest $W_{\%}$ in the case of the horn antenna is < 0.5 dB, whereas for the dual-frequency patch there is a difference < 1 dB between 46% and 50%, and < 0.5 dB between 50% and 54%, for both peaks.

Fig. 11a, on the other hand, shows the frequency response using the simple narrow-band coaxial-fed patch antenna. In this case, the difference in $W_{\%}$ is evident in the shift of the

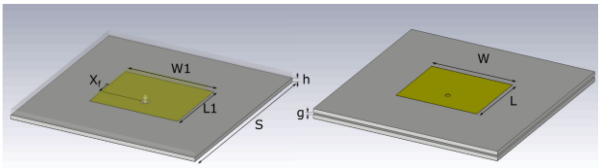

FIGURE 7. Dimensional drawing of the series fed stacked patch antenna. Parameters: $S = 50$ mm, $h = 1$ mm, $a_1 = 73.4$ mm, $W1 = 22$ mm, $L1 = 18.25$ mm, $x_f = 4.8$ mm, $g = 0.5$ mm, $W = 24$ mm, $L = 18.5$ mm.

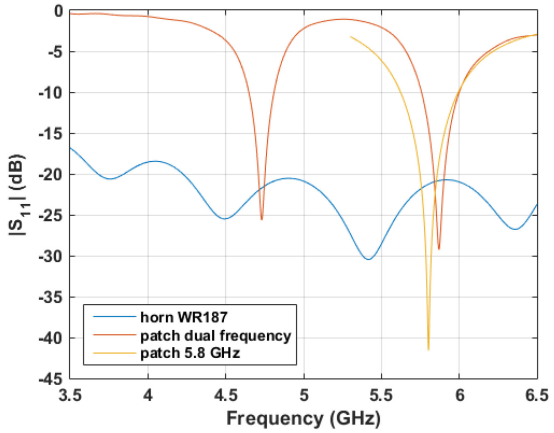

FIGURE 8. Comparison between the simulated S_{11} magnitude of the wide-band horn, the dual-band patch, and the 5.8 GHz patch antennas in free space.

S_{11} magnitude minima, with lower minima corresponding to higher water content. Upon further inspection it is clear that the difference between the minima corresponding to each $W_{\%}$ is about 5 dB. The different sensitivity of the three layouts has been summarized in Table 1. This difference can be regarded as a matching difference due to the change in complex permittivity (which is obviously tied to the different $W_{\%}$). Indeed, the 5.8 GHz rectangular patch antenna used as a sensor is a simplistic layout but very well matched with the 50 Ω feeding in free space, as shown in Fig. 8. Very good matching is maintained also for high water contents (i.e., 54%, see Fig. 11a), whereas it worsens slightly as the water content lowers (see also Section V in the supplementary material).

An additional investigation on the S_{11} phase shows that its trend is barely affected by the water percentage when using the 5.8 GHz patch (see Fig. 11b), a piece of information that is going to be significant in the next steps of the study. This proves, at least numerically, that a simple patch antenna could be used for the discrimination of the $W_{\%}$ inside the dough. A representation of the simulation environment is reported in Fig. 12 (the model is the same used also for the other antenna layouts).

V. EARLY PROTOTYPE FABRICATION AND EXPERIMENTAL MEASUREMENTS

The simulations provided a hint that a simple patch antenna working at 5.8 GHz might be capable of discriminating small percentage variations of water content inside the sheeted

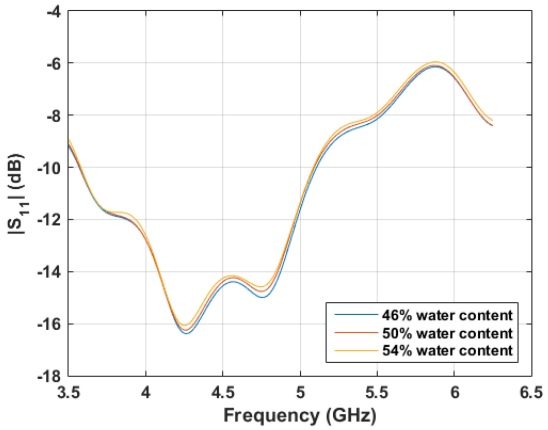

FIGURE 9. Simulated magnitude of the S_{11} for the wide-band horn antenna placed at d = 10 mm, for different water contents.

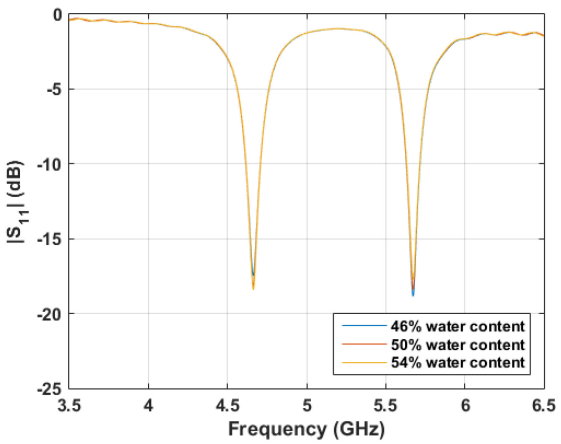

FIGURE 10. Simulated magnitude of the S_{11} for the dual-band patch antenna placed at d = 10 mm, for different water contents.

TABLE 1. Sensitivity of the presented layouts with respect to the W% variation, evaluated as difference in the |S11| minima.

min $\lvert S_{11}\rvert$	from 46 % to 50%	from 50% to 54%
WR 187 Horn	< 0.25 dB	< 0.25 dB
Series-fed stacked patch	< 0.5 dB	< 1 dB
5.8 GHz patch	~ 5 dB	~ 5 dB

Carasau bread dough. This assumption is, nonetheless, based mainly on the observed difference of about 5 dB in S_{11} magnitude minima within a numerical simulation. Actually, this information could be lost in a real measurement, as this matching difference might not be relevant in absence of the "ideal" context provided by the simulation. Indeed, to validate this finding a real case scenario must be tested, hence, an *ad hoc* measurement setup has been designed. Three different doughs with the targeted $W_{\%}$ (46%, 50%, and 54%) have been prepared and, after kneading and a first leavening, have been sheeted to obtain small samples for the measurements. The samples have been sheeted using a pasta machine, to reach a thickness of about 1 mm. It must be noticed that such small samples have not the same size

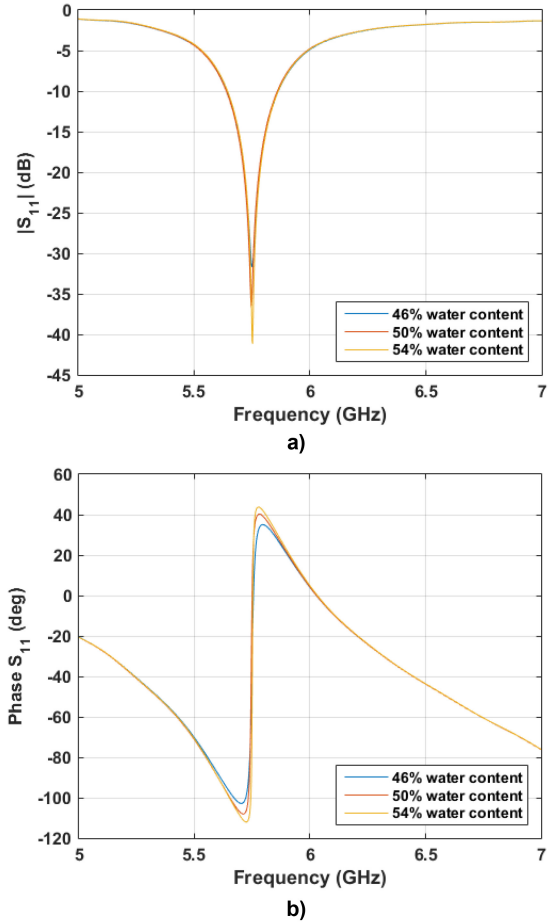

FIGURE 11. Simulated magnitude (a) and phase (b) of the S_{11} for the 5.8 GHz patch antenna placed at d = 10 mm, for different water contents.

of the disks used in the numerical simulations, for practical reasons. However, this does not affect the frequency response of the antenna, since the edges of the sheeted samples are still far enough from the sensor. The measurement setup consists of:

- a laser sensor (optoNCDT ILD 1900-2 from Micro-epsilon) employed to determine the thickness of the sheeted samples and the distance of the antenna from the sheet;
- the 5.8 GHz patch antenna described in Section IV, employed as a water content sensor;
- a custom 3D printed PLA arm with interchangeable housing for the laser sensor and the antenna;
- a metallic support to adjust the plastic arm height;
- a 3D printed PLA plate to lay down the sheeted sample;
- a commercial VNA (Hewlett-Packard 8720C) with frequency range from 5 to 7 GHz, number of points equal to 801 (which is equivalent to a frequency resolution of about 2.5 MHz), system dynamic range equal to 103 dBm and input power equal to 10 dBm.

A picture of the described setup is shown in Fig. 13. The measurements have been performed in a dedicated laboratory at room temperature (~26°C). The precise thickness of the sheeted dough measured with the laser was 1.165 mm,

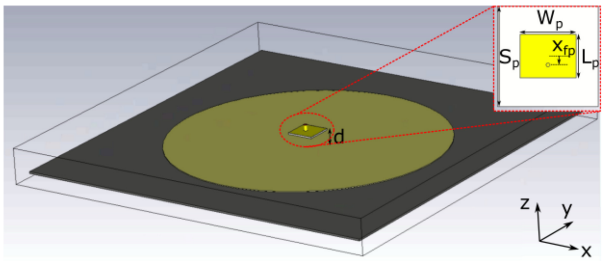

FIGURE 12. Representation of the simulation environment with the simple 5.8 GHz patch antenna (the same model is used for all the layouts). Parameters: $S_p = 35$ mm, $W_p = 19.54$ mm, $L_p = 15.15$ mm, $x_{fp} = 3$ mm, $h_p = 2$ mm (substrate thickness), $d = 10$ mm.

whereas the default measured distance of the antenna from the sheet was 34 mm. This value is not the same one used in the simulation, but the two environments greatly differ from each other, in the first place, and, secondly, the measurement antenna-sheet distance value has been chosen in order to obtain the best impedance matching (RL > 20 dB) for the standard dough ($W_{\%}$= 50%). The rationale is that spotting the predicted 5 dB difference between the different water content would be much easier starting from a well matched frequency response, as in the case of the simulations.

The measured frequency response, both in magnitude and phase, of the described environment, is reported in Fig. 14. As it can be seen from the image, the shift in $|S_{11}|$ minima due to the variation of $W_{\%}$ can be appreciated also from these results, and quite surprisingly, there is a difference of about 5 dB, in agreement with what the simulations have produced. The similarity does not stop to the magnitude analysis, as also the phase shows a common trend in the measurements, just like the numerical simulations, thus demonstrating the validity and suitability of the proposed moisture content measurement method. The presented antenna, despite being simplistic in nature and probably not perfectly suitable as a definitive layout employed in the real industrial application, is a rather promising prototype that successfully demonstrate the proof-of-concept of a methodology tied to the Carasau industry and the Carasau dielectric profile. It is not intended as a test plan for the industrial integration, lacking the operating structure effectively employed for the bread production. Still, a general agreement between simulations and measurements is a right step forward for a real industrial application, which may employ a layout not drastically different from the one herein described.

It would be useful to define a Figure of Merit (FoM) for the presented problem, able to quantify the performance of the sensor antenna. The most useful information, as already discussed previously, is the $|S_{11}|$ minima variation with respect to the $W_{\%}$ variation. A difference of about 5 dB can be seen from both simulations and measurements. Thus, we can define a FoM as it follows:

$$F = \frac{\Delta(min|S_{11}|)}{\Delta W_{\%}} \tag{1}$$

wherein $\Delta(min|S_{11}|)$ is the difference, in dB, between the $|S_{11}|$ minima for different $W_{\%}$ and $\Delta W_{\%}$ is the difference in water percentage of the dough. Using this formulation, for the presented case, we obtain F = 1.25 dBppp (decibel per percentage point). Additionally, if we consider a difference of about 3 dB (half power) as the minimum acceptable difference, we can also define a lower limit of F, in order to establish the suitability of a sensor for the same purpose as the one herein presented. In this case, we have:

$$F \geq 0.75\ dBppp \tag{2}$$

On a note of a possible configuration that could be used in a real operating industrial setting, the presented system could be easily integrated in the production chain, taking advantage of a mounting structure, above the conveyor belt, in which the sensor could be located. To help the visualization of this system, a conceptual drawing has been reported in Fig. 15. The sensor should consist of more than one antenna in single mode operation (not an array), in order to map the entirety of the dough sheet (each antenna "illuminates" a different portion of the sample), at an optimal distance d from the sheeted dough, in order to have a good matching. The antennas should be simply displaced in a linear fashion along the y-direction, as we can take advantage of the conveyor belt movement in the x-direction, with reference to the drawing of Fig. 15. The sensor should be connected to a small VNA (e.g., a Nano-VNA) or an electronic board able to fulfill the same functions (e.g., like an FPGA), which, in turn, should be connected to a system for the information processing. Further insights on the latter topic can be found in Section VII. We would like to stress out that the Hewlett-Packard 8720C VNA used in the presented measurements is an old and bulky model and it was employed only for validation purposes, but it would result unsuitable for a real-case scenario. In fact, within the described system of Fig. 15, given the speed of the conveyor belt (from few to tens of m/s) and the distance from two consecutive dough sheets, at steady state, an arbitrary section of the conveyor belt can be crossed by 1 dough sheet every 2 seconds. The sweep time of the employed VNA (with the provided frequency span and number of points) is equal to 2.408 seconds, thus it would be unable to perform even one full acquisition in a real scenario. However, today more compact and performing VNAs are available commercially that are more than capable to handle multiple data acquisitions in a time frame of 2 seconds.

VI. RECOGNITION OF EXTERNAL FACTORS

In addition to the presented analysis, a further study has been carried out to investigate possible sources of misinterpretation of the results. In particular, two effects that could be detrimental for the main purpose of the water content sensor are some changes in the geometry of the setup herein used for the measurements. It must be absolutely clear that these events are highly unlike to happen to an extent that could be troubling, but take them into due account is a dutiful part of a comprehensive uncertainty analysis, to

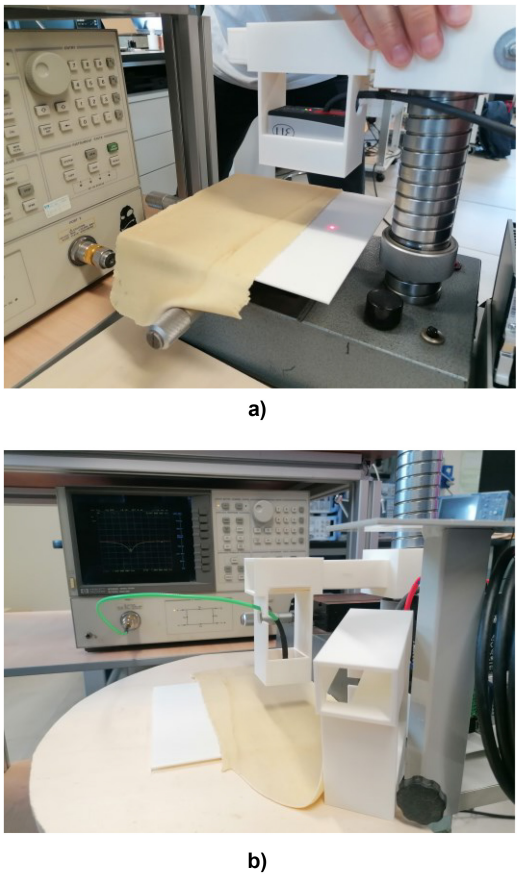

FIGURE 13. Picture of the employed measurement setup with the laser sensor attachment (a) and the water content sensor attachment (b).

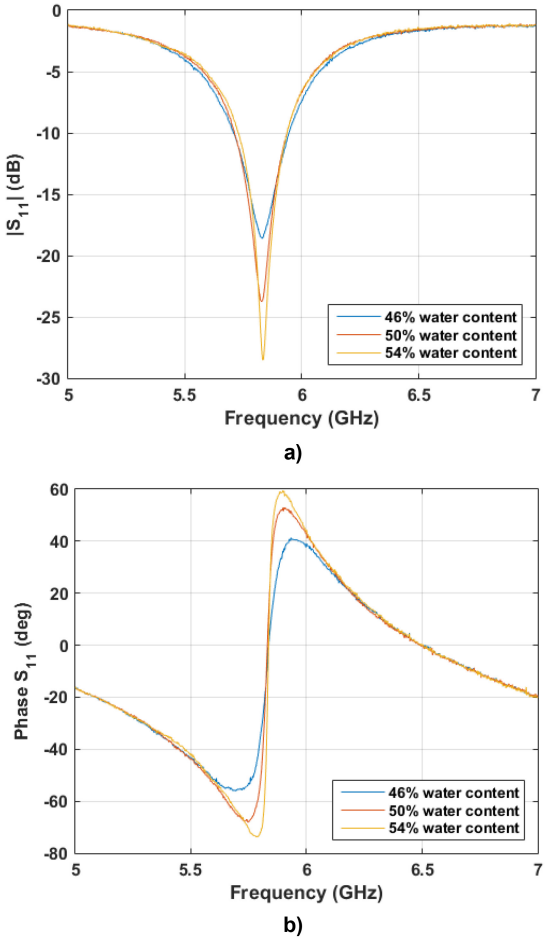

FIGURE 14. Measured magnitude (a) and phase (b) of the S_{11} for the 5.8 GHz patch antenna placed at $d = 10$ mm, for different water contents.

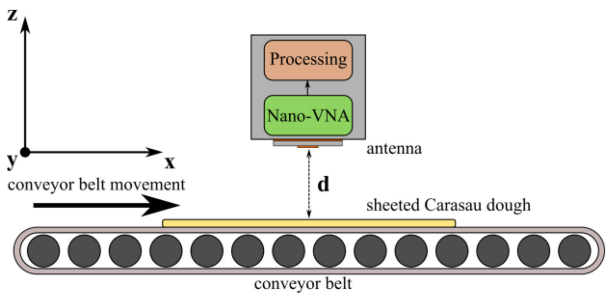

FIGURE 15. Conceptualization of a possible implementation of the moisture sensing system in a real industrial scenario.

clearly set the reliable operative conditions of the proposed sensor. The two effects that we are going to consider in the following discussion are the change of the antenna-sheet distance d and the change of the sheet thickness h_s, and if the variation of these quantities could be a possible source of confusion when compared to the water content variation.

As in the case of water content variation, to address these points, a preliminary simulation (with the same environment described in Section IV) is carried out, followed by a measurement validation. In this respect, in Fig. 16, the simulated magnitude and phase of the S_{11} when accounting for an antenna-sheet distance d varying between 5 and 15 mm (for the sake of clarity the $W_{\%}$ has been kept equal to 50% and the sheet thickness h_s equal to 1 mm) is shown. The translation of the $|S_{11}|$ minima is visible also in this case but it is paired with a large frequency shift in the order 60-70 MHz (compare Fig. 16a with Fig. 11a). Since the $|S_{11}|$ minima frequency shift, as we already pointed out, is not ascribable to the variation of the $W_{\%}$, this is a clear effect of the variation of the antenna-sheet distance. Additionally, the S_{11} phase appears highly dependent from the distance d (see Fig. 16b) and there is no common trend in the phase curves. This does not happen in the case of varying $W_{\%}$, wherein the phase trend remains stable, so it can be a good indicator of the real cause behind the $\min(|S_{11}|)$ shift. In the same fashion, in Fig. 17, the frequency response for the sheet thickness (h_s) variation between 1 and 2.5 mm is reported (with $W_{\%}$ fixed to 50%). In this case, there is a change in $|S_{11}|$ minima but not a frequency shift, picturing a situation similar to the $W_{\%}$ variation.

However, the phase curves do not match (compare Fig. 17b with Fig. 11b), and, as in the case of the distance variation, this discrepancy can be used to discriminate the two effects ($W_{\%}$ variation from h_s variation).

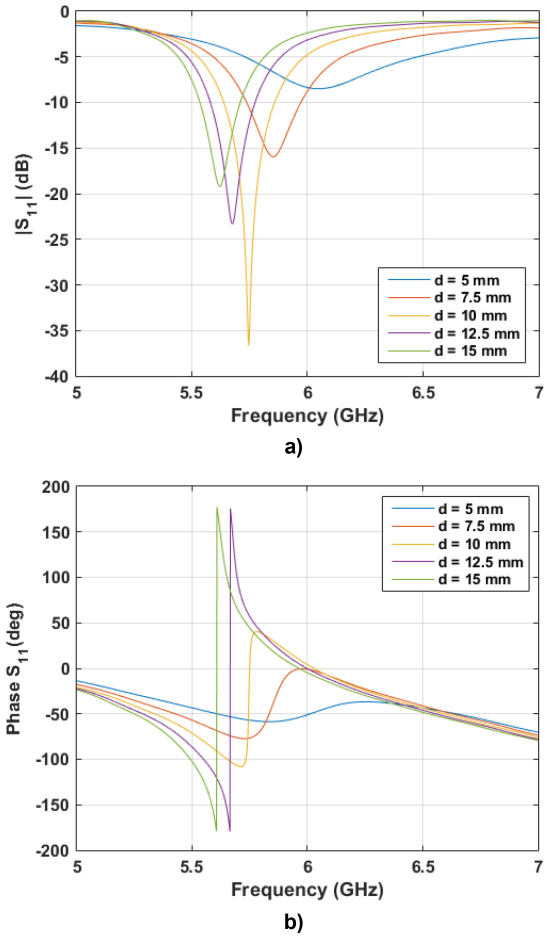

FIGURE 16. Simulated magnitude (a) and phase (b) of the S_{11} for the 5.8 GHz patch antenna for different values of d (water content fixed to 50%, h_s fixed to 1 mm).

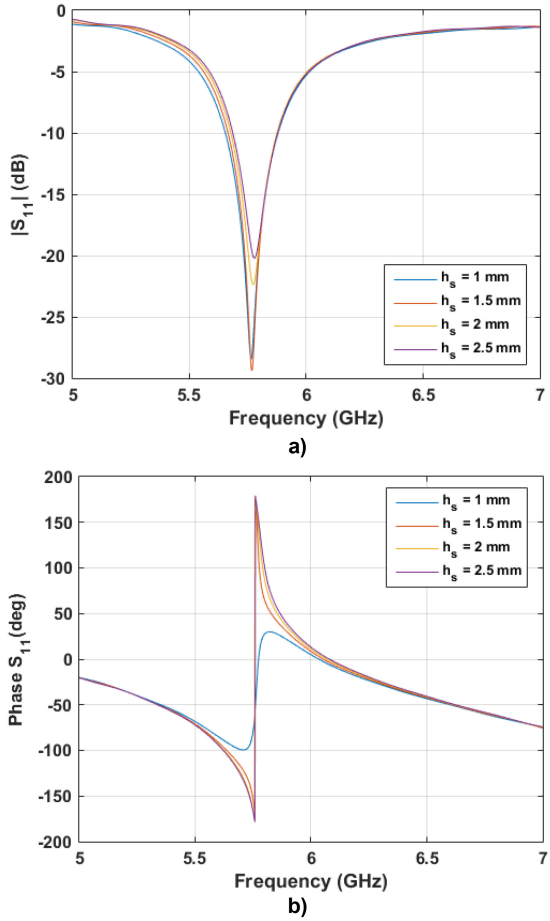

FIGURE 17. Simulated magnitude (a) and phase (b) of the S_{11} for the 5.8 GHz patch antenna for different values h_s (water content fixed to 50%).

The next step is to validate the presented simulations by real measurements, using the same setup described in Section V. As in the case of the numerical simulations, the distance d and thickness h_s are progressively increased by 2.5-mm and 0.5-mm steps, respectively (distances and thicknesses have been measured using the laser sensor). The measured S_{11} for the increment of the distance d is shown in Fig. 18. Again, it can be noticed the agreement between simulations and measurements, since the shift in both frequency and magnitude is still visible (in this case the frequency shift is in the order of 20-25 MHz but it is, nonetheless, important especially with respect to the unnoticeable shift experienced for the $W_{\%}$ variation). The same can be inferred for the phase, wherein no common trend with the default case is observed. Finally, in Fig. 19, the measured S_{11} for the increment of the thickness h_s is shown. While the $|S_{11}|$ pictures a similar situation to the simulation (change in magnitude but not in frequency), the information that allowed to discriminate this effect is lost in the phase, since a common trend is observed. This inconvenience might be due to the employment of non-conformal devices for the sheeting of the dough (we could achieve a 0.5 mm control on the dough thickness with the available pasta machine that is different from industrial sheeters) or to the elastic nature of the dough, whose relaxation and leavening cycles are still a subject for further study. Still, it must be remarked that these effects are taken to an extreme and while the proposed system is already capable of discriminating between water content and distance variation, the varying thickness problem could be solve with additional knowledge on the dough characteristics. In order to help the reader to navigate with ease through the presented results and findings, a summary table for quick comparison between simulated and measured results is reported in Fig. 20. The latter allows also to compare the frequency response of the antenna due to different effects. The summary is organized as follows: the rows (A, B, and C) are useful for a straight comparison of simulated and measured S_{11} (magnitude and phase) referred to a single factor, A for water content variation, B for antenna-sheet distance variation, and C for sheet thickness variation; the columns I, II, III, and IV allow a prompt comparison of the effect that each factor has on the frequency response of the antenna.

VII. CONCLUSION AND FUTURE PERSPECTIVES

To comply with the technological advancements that the food industry is facing, involving also small-scale activities,

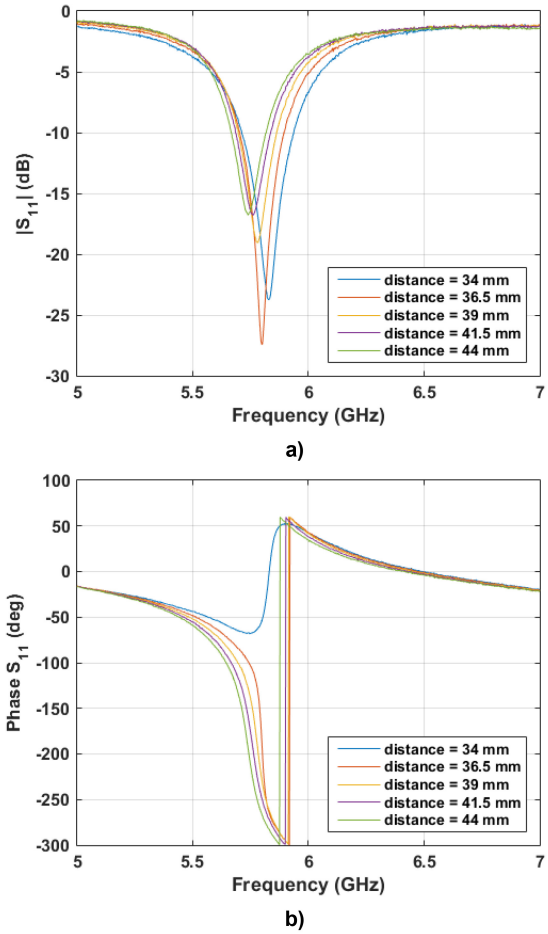

FIGURE 18. Measured magnitude (a) and phase (b) of the S_{11} for the 5.8 GHz patch antenna for different values of d (water content fixed to 50%, h_s fixed to 1 mm).

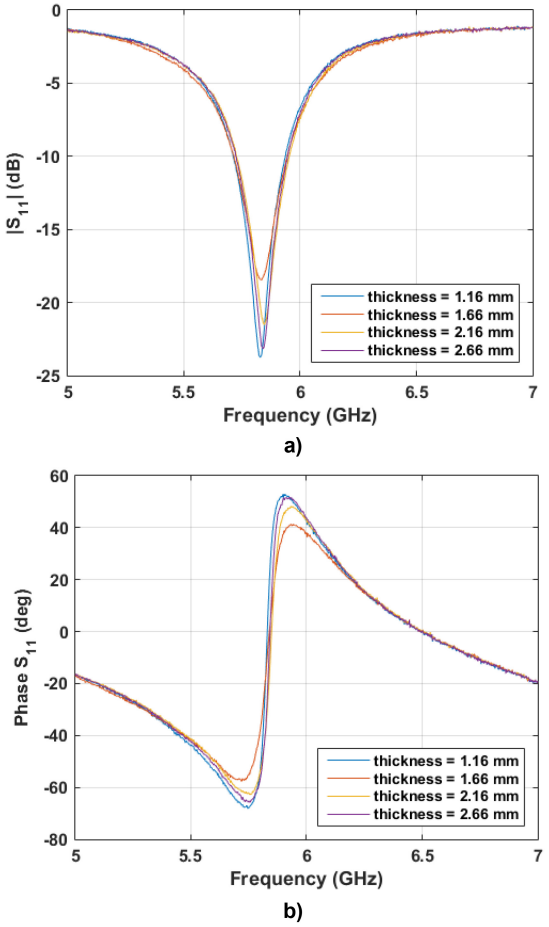

FIGURE 19. Measured magnitude (a) and phase (b) of the S_{11} for the 5.8 GHz patch antenna for different values h_s (water content fixed to 50%).

the design and early validation of a sensor for the water content estimation inside a typical Italian bread dough is herein presented. Carasau bread differs from classic bread in its shape and texture, thus needing an ad hoc system and a specific measurement methodology. Based on a survey on the operating conditions of a real bakery, the most important step within the production process lies between the second leavening and baking stages, wherein the water content inside the sheeted dough must be properly evaluated. An excessive or defective amount of water results in a flawed product that has to be discarded, affecting the economic returns of the production line. This raises the need of a contactless measurement and sensing procedure, with a device to be integrated in a fixed position above the conveyor belt, able to sense the different permittivity profile of every unbaked sheet that slides underneath.

Simulation results show that a narrow-band patch antenna is preferable to wide-band and dual-band counterparts. A simple contactless inline sensor is capable of discriminating small water percentage variations ($\sim 4\%$) inside the bread dough through the matching of the antenna response. This feature allows to monitor the water content inside the dough, avoiding defected products and wastes. The validation measurements confirm that the chosen antenna is capable of discriminating the water content. Additionally, a further study for the recognition of external factors that could undermine the discrimination of the water content variation has been presented. Based on the simulations, the chosen sensor is able to differentiate the effects unrelated to the water content, such as the variation of the antenna-sheet distance and the variation of the sheet thickness. These finding are confirmed also by the measurements, with regard to the antenna-sheet distance, whereas for the variation of sheet thickness further studies are needed.

Future work will deal with the specific usage of the information provided in the presented study. It could involve inversion algorithms of the scattering matrix, thus opting for the implementation of a microwave imaging system to map the moisture of the bread sheet with more accuracy, or a large database construction for a machine learning algorithm training. The presented contactless measurement methodology could also be applied to other food products with characteristic akin to those of the Carasau bread (thus, that undergo a baking step such as common bread, pastry, and so on) and other industrial processing scenarios calling for innovation.

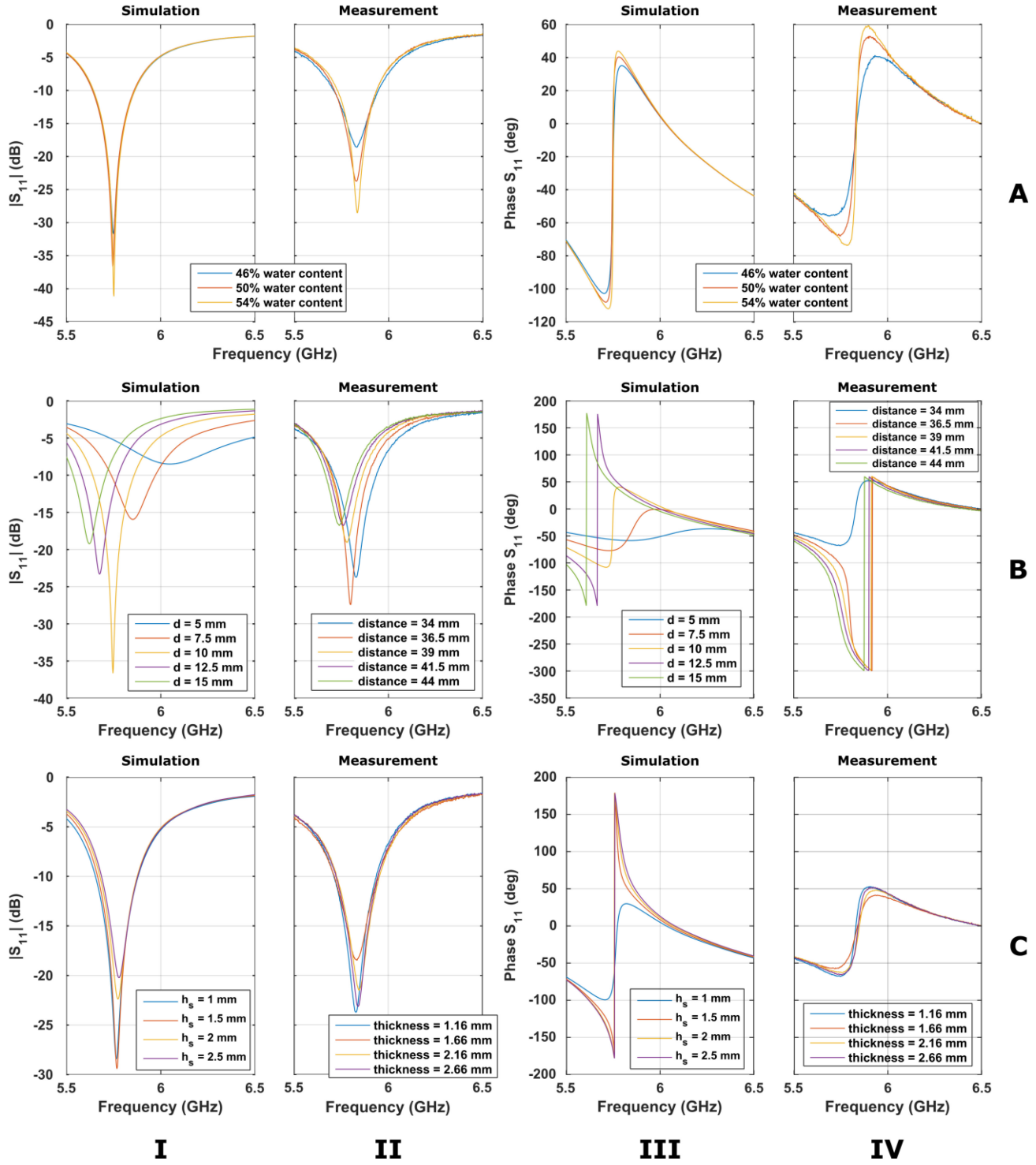

FIGURE 20. Summary of the simulated and measured results taking account for shift of magnitude and phase of the S_{11} due to the variation of water content $W_{\%}$, antenna-sheet distance d, and sheet thickness h_s.

ACKNOWLEDGMENT

The authors would like to express their thanks Massimo Bauco and Luigi Lorusso from the Rohde & Schwarz Italia for the VNA freely provided.

REFERENCES

[1] S. O. Nelson and P. G. Bartley, "Measuring frequency- and temperature-dependent permittivities of food materials," *IEEE Trans. Instrum. Meas.*, vol. 51, no. 4, pp. 589–592, Aug. 2002.

[2] N. Javanbakht, G. Xiao, and R. E. Amaya, "Portable microwave sensor based on frequency-selective surface for grain moisture content monitoring," *IEEE Sens. Lett.*, vol. 5, no. 11, pp. 1–4, Sep. 2021.
[3] T. Limpiti and M. Krairiksh, "In situ moisture content monitoring sensor detecting mutual coupling magnitude between parallel and perpendicular dipole antennas," *IEEE Trans. Instrum. Meas.*, vol. 61, no. 8, pp. 2230–2241, Mar. 2012.
[4] T. Tantisopharak, H. Moon, P. Youryon, K. Bunya-Athichart, M. Krairiksh, and T. K. Sarkar, "Nondestructive determination of the maturity of the durian fruit in the frequency domain using the change in the natural frequency," *IEEE Trans. Antennas Propag.*, vol. 64, no. 5, pp. 1779–1787, May 2016.
[5] S. Karuppuswami, A. Kaur, H. Arangali, and P. Chahal, "A hybrid magnetoelastic wireless sensor for detection of food adulteration," *IEEE Sens. J.*, vol. 17, no. 6, pp. 1706–1714, Mar. 2017.
[6] J. A. T. Vásquez et al., "Noninvasive inline food inspection via microwave imaging technology: An application example in the food industry," *IEEE Antennas Propag. Mag.*, vol. 62, no. 5, pp. 18–32, Aug. 2020.
[7] M. Ricci, J. A. T. Vasquez, R. Scapaticci, L. Crocco, and F. Vipiana, "Multi-antenna system for in-line food imaging at microwave frequencies," *IEEE Trans. Antennas Propag.*, vol. 70, no. 8, pp. 7094–7105, Aug. 2022.
[8] F. Gandino, B. Montrucchio, M. Rebaudengo, and E. R. Sanchez, "On improving automation by integrating RFID in the traceability management of the agri-food sector," *IEEE Trans. Ind. Electron.*, vol. 56, no. 7, pp. 2357–2365, Jul. 2009.
[9] I. Cuiñas, R. Newman, M. Trebar, L. Catarinucci, and A. A. Melcon, "RFID-based traceability along the food-production chain [Wireless Corner]," *IEEE Antennas Propag. Mag.*, vol. 56, no. 2, pp. 196–207, Apr. 2014.
[10] F. Paschino, F. Gabella, F. Giubellino, and F. Clemente, "The level of automation of 'carasau' bread production plants," *J. Agric. Eng.*, vol. 38, no. 2, pp. 61–64, 2007.
[11] M. Baire, A. Melis, M. B. Lodi, L. Lodi, A. Fanti, and G. Mazzarella, "Empowering traditional carasau bread production using wireless sensor network," in *Proc. IEEE Int. Symp. Circuits Syst. (ISCAS)*, Daegu, South Korea, 2021, pp. 1–4.
[12] L. Cocco et al., "A blockchain-based traceability system in agri-food SME: Case study of a traditional bakery," *IEEE Access*, vol. 9, pp. 62899–62915, 2021.
[13] G. Muntoni et al., "Designing a microwave moisture content sensor for carasau bread: A feasibility study," in *Proc. 16th Eur. Conf. Antennas Propag. (EuCAP)*, Madrid, Spain, 2022, pp. 1–4.
[14] F. Fanari, I. Frau, F. Desogus, E. A. Scano, G. Carboni, and M. Grosso, "Influence of wheat varieties, mixing time and water content on the rheological properties of semolina doughs," *Chem. Eng. Trans.*, vol. 75, pp. 529–534, Jan. 2019.
[15] F. Fanari, F. Desogus, E. A. Scano, G. Carboni, and M. Grosso, "The effect of the relative amount of ingredients on the rheological properties of semolina doughs," *Sustainability*, vol. 12, no. 7, p. 2705, 2020.
[16] F. Fanari, I. F. Naue, F. Desogus, M. Grosso, and M. Wilhelm, "Durum wheat dough torque measurements: Characterization and study of the mixing process parameters as a function of water and salt amounts," *Chem. Eng. Trans.*, vol.87, pp. 205–210, Jul. 2021.
[17] F. Fanari, G. Carboni, F. Desogus, M. Grosso, and M. Wilhelm, "A chemometric approach to assess the rheological properties of durum wheat dough by indirect FTIR measurements," *Food Bioprocess Technol.*, vol. 15, no. 5, pp. 1040–1054, 2022.
[18] F. Fanari, C. Iacob, G. Carboni, F. Desogus, M. Grosso, and M. Wilhelm, "Broadband Dielectric Spectroscopy (BDS) investigation of molecular relaxations in durum wheat dough at low temperatures and their relationship with rheological properties," *LWT*, vol. 161, May 2022, Art. no. 113345.
[19] M. B. Lodi et al., "Microwave characterization and modeling of the carasau bread doughs during leavening," *IEEE Access*, vol. 9, pp. 159833–159847, 2021.
[20] M. Bogosanovich, "Microstrip patch sensor for measurement of the permittivity of homogeneous dielectric materials," *IEEE Trans. Instrum. Meas.*, vol. 49, no. 5, pp. 1144–1148, Oct. 2000.
[21] N. Javanbakht, G. Xiao, and R. E. Amaya, "A comprehensive review of portable microwave sensors for grains and mineral materials moisture content monitoring," *IEEE Access*, vol. 9, pp. 120176–120184, 2021.
[22] K. Sarabanid and E. Li, "Microstrip ring resonator for soil moisture measurements," *IEEE Trans. Geosci. Remote Sens.*, vol. 35, no. 5, pp. 1223–1232, Sep. 1997.
[23] M. J. Tiusanen, "Wideband antenna for underground soil scout transmission," *IEEE Antennas Wireless Propag. Lett.*, vol. 5, pp. 517–519, 2006.
[24] A. Cataldo, G. Monti, E. De Benedetto, G. Cannazza, and L. Tarricone, "A noninvasive resonance-based method for moisture content evaluation through microstrip antennas," *IEEE Trans. Instrum. Meas.*, vol. 58, no. 5, pp. 1420–1426, May 2009.
[25] P. Leekul, B. Mgawe, T. Kazema, H. N. Dao, P. Sirisuk, and M. Krairiksh, "Simple and effective design concept for constructing in-situ soil dielectric property sensor with dual low-cost COTS microwave modules," *IEEE Access*, vol. 10, pp. 54516–54524, 2022.
[26] R. Keshavarz, J. Lipman, D. M. M.-P. Schreurs, and N. Shariati, "Highly sensitive differential microwave sensor for soil moisture measurement," *IEEE Sens. J.*, vol. 21, no. 24, pp. 27458–27464, Dec. 2021.
[27] N. Hosseini and M. Baghelani, "Selective real-time non-contact multivariable water-alcohol-sugar concentration analysis during fermentation process using microwave split-ring resonator based sensor," *Sens. Actuators A, Phys.*, vol. 325, Jul. 2021, Art. no. 112695.
[28] S. Julrat and S. Trabelsi, "Influence of peanut orientation on microwave sensing of moisture content in cleaned unshelled peanuts," *IEEE Sens. J.*, vol. 22, no. 11, pp. 10515–10523, Jun. 2022.
[29] S. Jiarasuwan, K. Chamnongthai, and N. Kittiamornkul, "A design method for a microwave-based moisture sensing system for granular materials in arbitrarily shaped containers," *IEEE Sens. J.*, vol. 21, no. 17, pp. 19436–19452, Sep. 2021.
[30] M. M. Ghretli, K. Khalid, I. V. Grozescu, M. H. Sahri, and Z. Abbas, "Dual-frequency microwave moisture sensor based on circular microstrip antenna," *IEEE Sens. J.*, vol. 7, no. 12, pp. 1749–1756, Dec. 2007.
[31] N. Khalid, R. Mirzavand, H. Saghlatoon, M. M. Honari, and P. Mousavi, "A three-port zero-power RFID sensor architecture for IoT applications," *IEEE Access*, vol. 8, pp. 66888–66897, 2020.
[32] G. Gugliandolo, K. Naishadham, G. Neri, V. C. Fernicola, and N. Donato, "A novel sensor-integrated aperture coupled microwave patch resonator for humidity detection," *IEEE Trans. Instrum. Meas.*, vol. 70, pp. 1–11, Feb. 2021.
[33] L. Tebben, Y. Shen, and Y. Li, "Improvers and functional ingredients in whole wheat bread: A review of their effects on dough properties and bread quality," *Trends Food Sci. Technol.*, vol. 81, pp. 10–24, Nov. 2018.

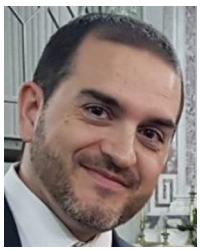

GIACOMO MUNTONI (Member, IEEE) graduated in electronic engineering and telecommunication engineering from the University of Cagliari in 2010 and 2015, respectively. He received the Ph.D. degree in electronic engineering and computer science from the University of Cagliari in 2019.

He is currently working as a Technologist with the Applied Electromagnetics Group, University of Cagliari. His research activity involves: design and characterization of antennas for biomedical and aerospace applications, microwave–based dielectric characterization of materials, 3-D printing of RF components, and monitoring of the space debris environment in low Earth orbit with the sardinia radio telescope, in collaboration with the Cagliari Astronomical Observatory.

MATTEO B. LODI (Member, IEEE) received the bachelor's degree in biomedical engineering from the University of Cagliari in 2016, the master's degree in biomedical engineering from the Politecnico di Torino in 2018, and the Ph.D. degree (with Hons.) in electronic engineering and computer science from the University of Cagliari in 2022.

He is currently working as a Research Assistant with the Applied Electromagnetics Group. His research activity deals with the modeling of bioelectromagnetic phenomena, especially hyperthermia treatment; the study, manufacturing, and synthesis of magnetic biomaterials for tissue engineering applications; and the use of microwaves for biotechnology and environmental applications, while working in the design and characterization of antennas for space and wearable applications. He has been awarded with the Roberto Sorrentino Young Scientist Award at the 2022 Italian URSI Assembly. He has been awarded as a Young Scientists at the General Assembly and Scientific Symposium of URSI in 2020 and 2021. He is a member of the WG2: "Better Thermal-Based EM Therapeutics" of the COST Action 17115 "MyWave". He has been appointed as the Chair of IEEE Nanotechnology Council Young Professionals.

ALESSANDRO FEDELI (Member, IEEE) received the B.Sc. and M.Sc. degrees in electronic engineering and the Ph.D. degree in science and technology for electronic and telecommunications engineering from the University of Genoa, Genoa, Italy, in 2011, 2013, and 2017, respectively, where he is currently an Assistant Professor with the Department of Electrical, Electronic, Telecommunications Engineering, and Naval Architecture. His research activities, carried out at the Applied Electromagnetics Laboratory, are mainly focused on the development and the application of computational methods for the solution of forward and inverse scattering problems, and electromagnetic imaging. He has coauthored more than 130 scientific contributions published in international journals and conference proceedings. He is a member of the IEEE Antennas and Propagation Society, the Italian Society of Electromagnetism, and the Interuniversity Center for the Interaction between Electromagnetic Fields and Biosystems.

ANDREA MELIS received the bachelor's degree in biomedical engineering from the University of Cagliari, Italy, in 2017, where he worked as an Assistant Researcher. His research interests include EM modeling and development of RF coils at low and high frequencies, especially for MRI at high field, the design and realization of WSN systems for the monitoring of industrial processes, such as bread manufacturing and intelligent transportation systems.

CLAUDIA MACCIÒ received the bachelor's and master's degrees in physics from the University of Cagliari, Cagliari, Italy, in 2015 and 2018, respectively, where she is currently pursuing the Ph.D. degree in electronic engineering and computer science. Following graduation, she also attended a oneyear training course for mechatronics experts with POEMA srl, a spin-off company of the Italian National Institute Astrophysics (INAF), receiving research grants from INAF and the University of Cagliari. Her research interests include the use of microwave for material characterization, in particular for food industry applications, design of microwave devices, structures and sensors, and innovative manufacturing process for microwave devices, such as 3-D printing and electroplating.

MATTEO PASTORINO (Fellow, IEEE) was a Full Professor of Electromagnetic Fields with the University of Genoa, Genoa, Italy, where he was the Director of the Department of Electrical, Electronic, Telecommunications Engineering, and Naval Architecture. He had coauthored about 500 articles in international journals and conference proceedings. His research interests include microwave and millimeter wave imaging, direct and inverse scattering problems, industrial and medical applications, smart antennas, and analytical and numerical methods in electromagnetism. He was an Associate Editor of the *IEEE Antennas and Propagation Magazine* and IEEE OPEN JOURNAL OF ANTENNAS AND PROPAGATION. He was the Chair of the National URSI Commission B (Fields and Waves), and the Vice Director of the Interuniversity Center for the Interaction between Electromagnetic Fields and Biosystems.

ANDREA RANDAZZO (Senior Member, IEEE) received the Laurea degree in telecommunication engineering and the Ph.D. degree in information and communication technologies from the University of Genoa, Genoa, Italy, in 2001 and 2006, respectively, where he is currently a Full Professor of Electromagnetic Fields with the Department of Electrical, Electronic, Telecommunication Engineering, and Naval Architecture. He has coauthored the book *Microwave Imaging Methods and Applications* (Artech House, 2018) and more than 270 articles published in journals and conference proceedings. His primary research interests are in the field of microwave imaging, inverse-scattering techniques, numerical methods for electromagnetic scattering and propagation, electrical tomography, and smart antennas.

GIUSEPPE MAZZARELLA (Senior Member, IEEE) received the degree (summa cum laude) in electronic engineering from the Università Federico II of Naples in 1984, and the Ph.D. degree in electronic engineering and computer science in 1989. In 1990, he became an Assistant Professor with the Dipartimento di Ingegneria Elettronica, Università Federico II of Naples. Since 1992, he has been with the Dipartimento di Ingegneria Elettrica ed Elettronica, Università di Cagliari first as an Associate Professor and then, since 2000 has been a Full Professor, teaching courses in electromagnetics, microwave, antennas and remote sensing. He is the author (or a coauthor) of over 100 articles in international journals and a reviewer for many EM journals. His research interests include the efficient design of large arrays of slots, power synthesis of array factor, with emphasis on inclusion of constraints, microwave holography techniques for the diagnosis of large reflector antennas, use of evolutionary programming for the solution of inverse problems, in particular problems of synthesis of antennas and periodic structures, agrifood, and therapeutic applications of microwaves.

ALESSANDRO FANTI (Senior Member, IEEE) received the Laurea degree in electronic engineering and the Ph.D. degree in electronic engineering and computer science from the University of Cagliari, Cagliari, Italy, in 2006 and 2012, respectively.

From 2013 to 2016, he was a Postdoctoral Fellow with the Electromagnetic Group, University of Cagliari, where he was an Assistant Professor of Electromagnetic Fields with the Department of Electrical and Electronic Engineering, from March 2017 to March 2024. He is currently an Associate Professor with the University of Cagliari. He has authored or coauthored 70 articles in international journals. From 2020 to 2023, he had been acting as a Principal Investigator of the IAPC Project, which was funded with five million euros by Italian Ministry of Economic Development (MISE), within the AGRIFOOD PON I&C (2014–2020). Since 2024, he has been acting as a Principal Investigator of the AISAC Project funded with 15 million euros by the Italian Ministry of Enterprises and Made in Italy, within the "ACCORDI PER L'INNOVAZIONE" (2021–2026). His research interests include the use of numerical techniques for modes computation of guiding structures, optimization techniques, analysis and design of waveguide slot arrays, analysis and design of patch antennas, radio propagation in urban environment, modeling of bioelectromagnetic phenomena, and microwave exposure systems for biotechnology and bioagriculture. He is also an Associate Editor of the IEEE JOURNAL OF ELECTROMAGNETICS, RF AND MICROWAVES IN MEDICINE AND BIOLOGY. He is a member of the IEEE Antennas and Propagation Society, Italian Society of Electromagnetism, National Inter-University Consortium for Telecommunications, and Interuniversity Center for the Interaction Between Electromagnetic Fields and Biosystems.

Open Access funding provided by 'UniversitÃ degli Studi di Cagliari' within the CRUI CARE Agreement